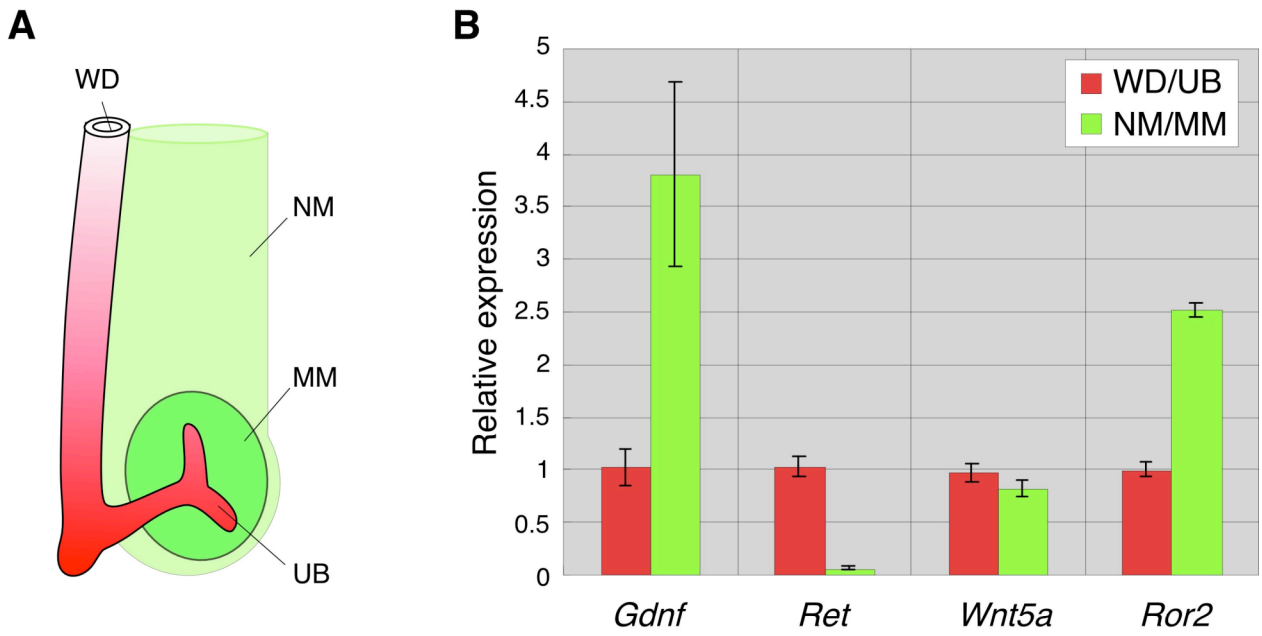

Figure S1. Quantitative RT-PCR analysis for *Wnt5a* and *Ror2*. (A) A schematic diagram of kidney tissues at E11.5. WD, Wolffian duct; UB, ureteric bud; NM, nephrogenic mesenchyme; MM, metanephric mesenchyme. (B) The kidney epithelia (WD and UB) and mesenchymes (NM and MM) were separated and subjected to quantitative RT-PCR analysis for *Wnt5a* and *Ror2*. *Gdnf* and *Ret* were also measured as markers for the MM and WD/UB, respectively.

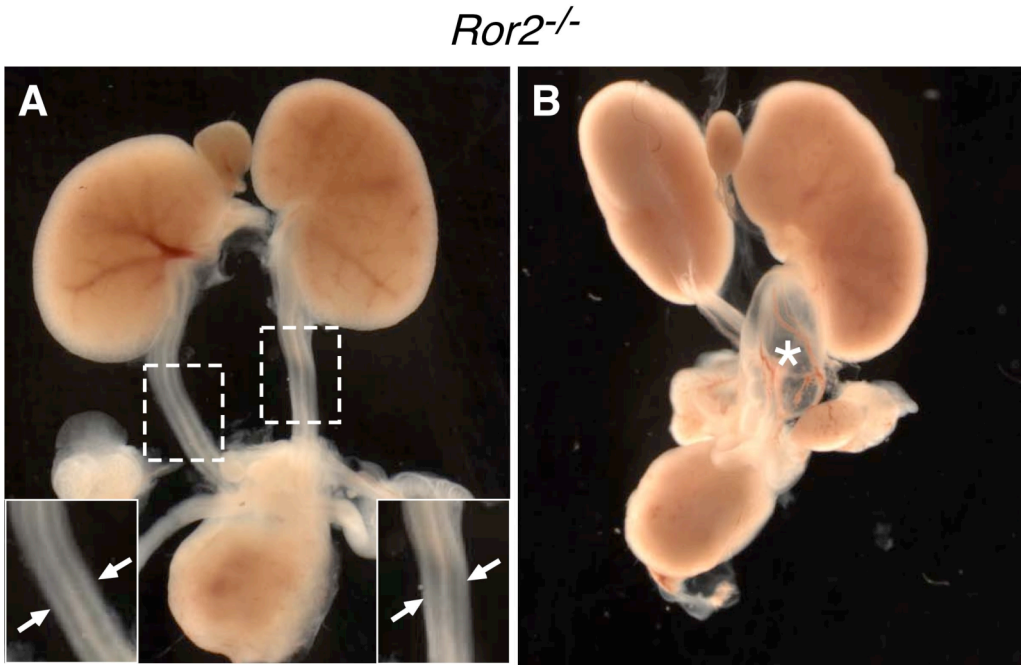

Figure S2. Bilateral duplicated ureters (A) and hydroureter (B) observed in *Ror2*-deficient embryos at E18.5. The insets in (A) show magnified views of the boxed regions with duplicated ureters (arrows). The asterisk in (B) indicates hydroureter.

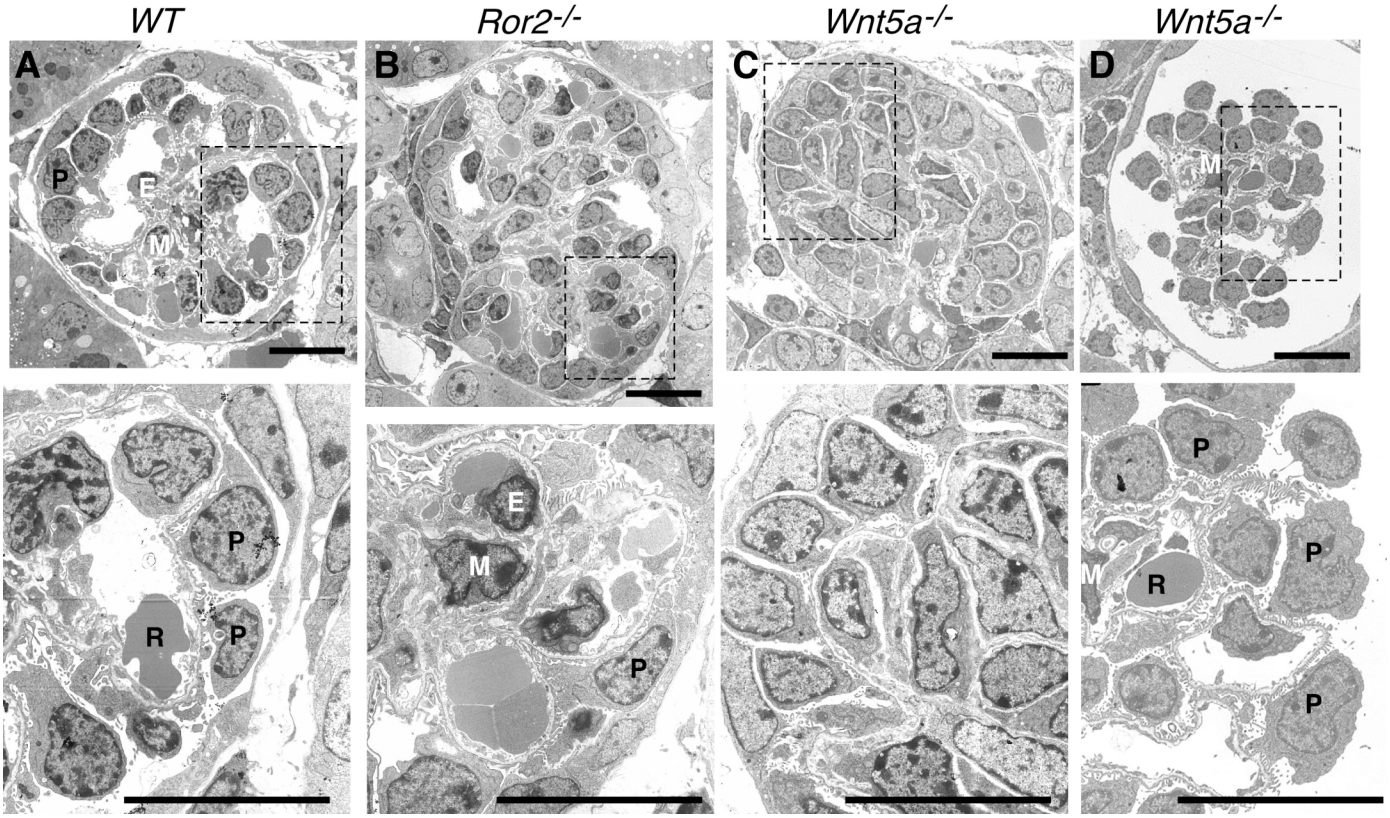

Figure S3. Transmission electron microscopy of the renal corpuscles in wild-type kidneys (A), *Ror2*$^{-/-}$ kidneys (B), and *Wnt5a*$^{-/-}$ kidneys with (C) and without (D) severe hydronephrosis at E18.5. Lower panels show high magnification view of the boxed region in the upper panels. E, endothelium; P, podocyte; R, red blood cell; M, mesangial cell. Size bar, 10 μm.

A

Genotype	Kidney phenotypes		
	Single ureter	Double ureter	Agenesis
Ror2$^{+/-}$;*Wnt5a*$^{+/-}$ (n=7)	7	0	0
Ror2$^{-/-}$;*Wnt5a*$^{+/+}$ (n=5)	3	2[a]	0
Ror2$^{-/-}$;*Wnt5a*$^{+/-}$ (n=7)	1	2[a]	4[b]

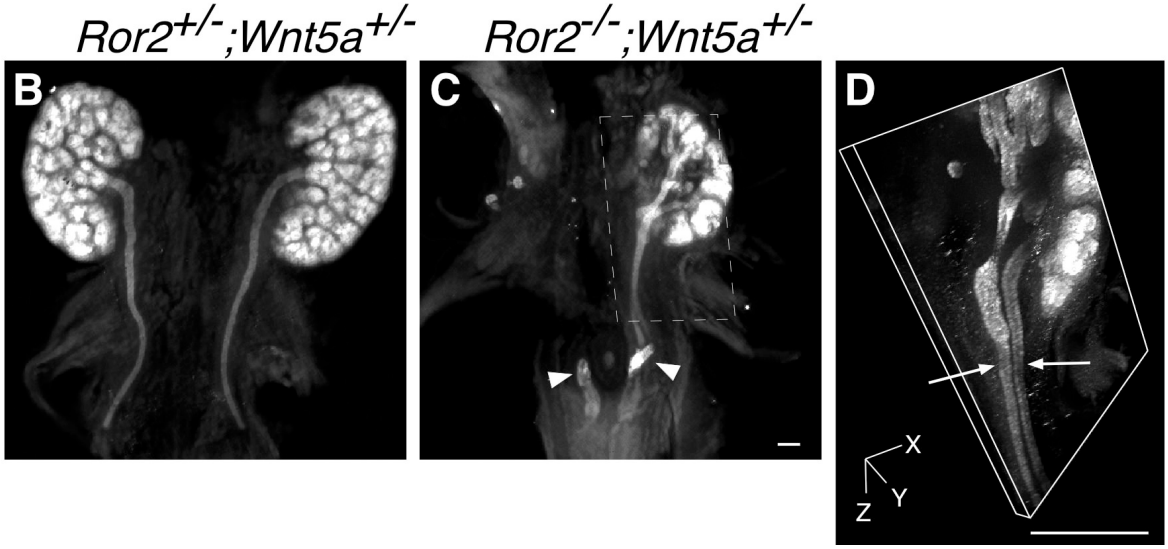

Figure S4. Genetic interactions between *Wnt5a* and *Ror2* during kidney development. Kidneys were isolated from embryos at E12.5 and subjected to anti-Pax2 whole-mount immunostaining. (A) The data represent the number of the embryos with the indicated kidney phenotypes. [a]All exhibited unilateral double ureter. [b]1 exhibited bilateral agenesis, 2 exhibited unilateral agenesis with single ureter on contralateral kidney, and 1 exhibited unilateral agenesis with double ureters in the contralateral kidney as shown in (C) and (D). (B) *Ror2*$^{+/-}$;*Wnt5a*$^{+/-}$ kidneys with single ureter on either side. (D) shows the 3D image of the boxed region in (C). The arrowheads and arrows indicate the Wolffian duct stumps and ureters, respectively.

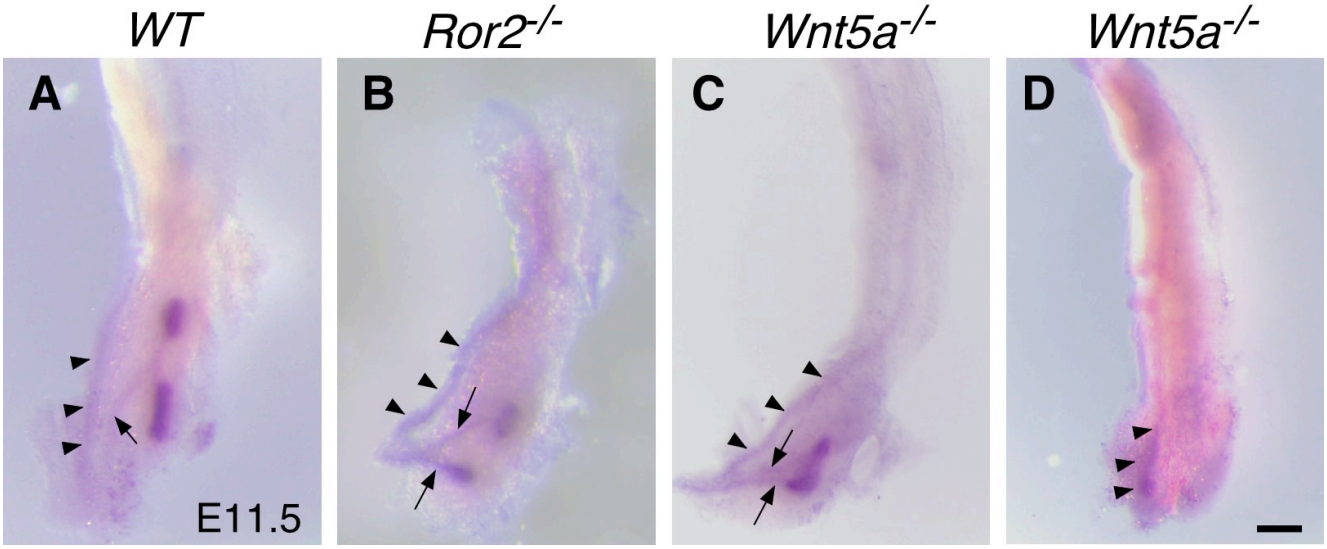

Figure S5. *Ret* expression is unaffected in *Ror2*- and *Wnt5a*-deficient kidneys. Whole-mount *in situ* hybridization of kidneys (E11.5) with *Ret* anti-sense probe, showing its expression in the WD (arrowheads) and duplicated UBs (arrows) in *Ror2*$^{-/-}$ (B) and *Wnt5a*$^{-/-}$ (C) kidneys. *Ret* is also detected in the WD in *Wnt5a*$^{-/-}$ kidneys without UB outgrowth (D).

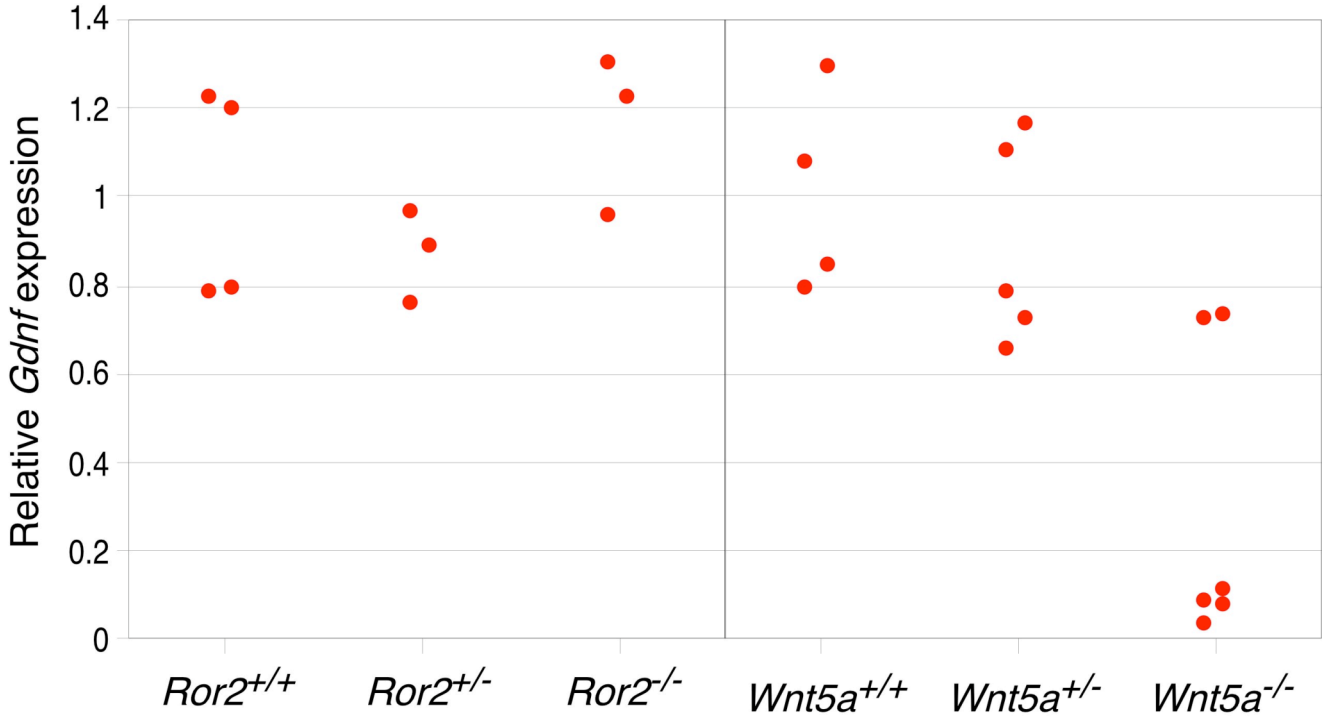

Figure S6. Quantitative RT-PCR analysis for *Gdnf* in *Ror2*- and *Wnt5a*-deficient kidneys. Kidneys were isolated form embryos with the indicated genotypes at E11.0 and subjected to quantitative RT-PCR analysis for *Gdnf*. Note that *Gdnf* expression is hardly detected in some *Wnt5a*$^{-/-}$ embryos (4 out of 6).

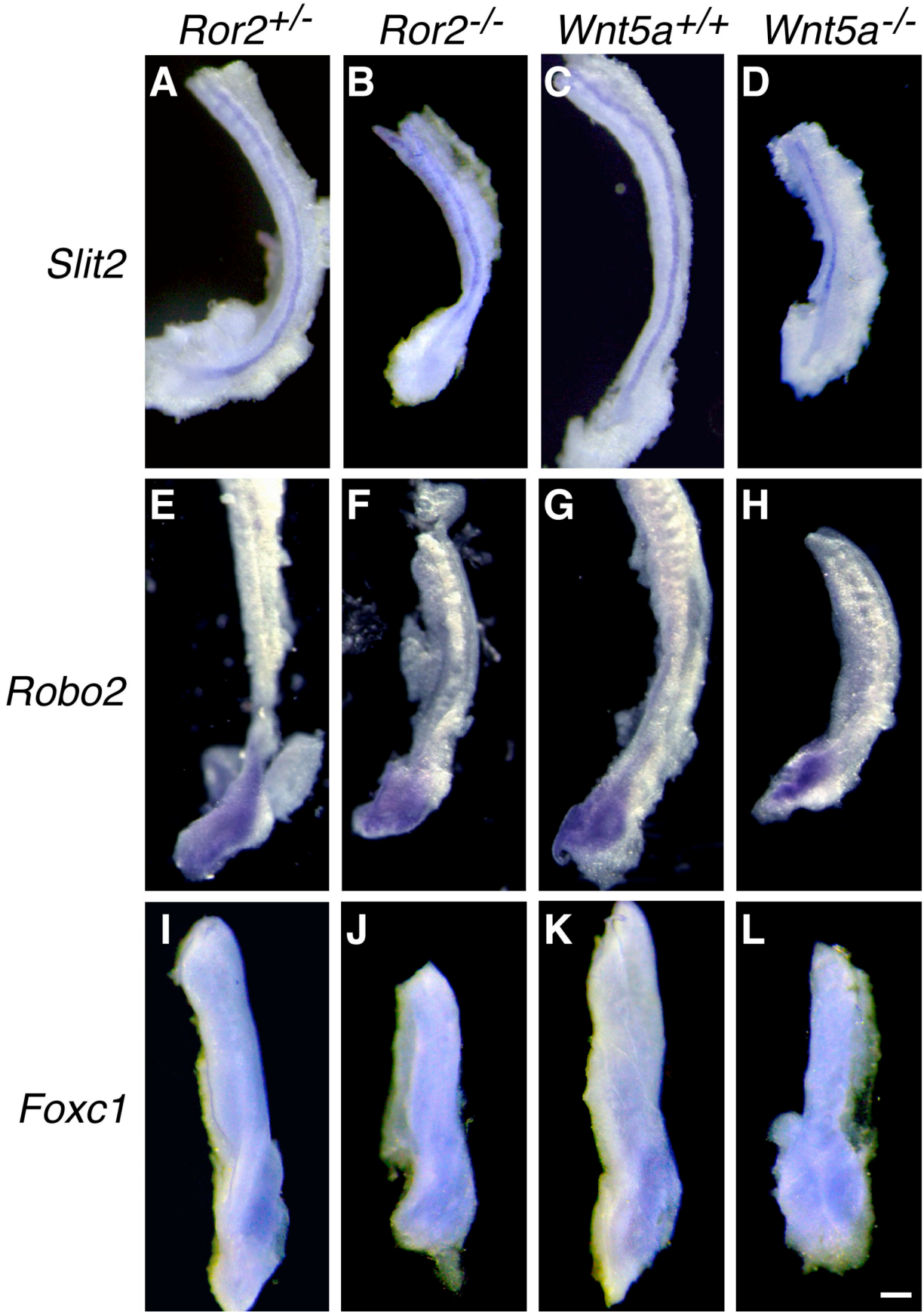

Figure S7. Expression of *Slit2, Robo2, and Foxc1* is unaffected in *Ror2*- and *Wnt5a*-deficient kidneys. Whole-mount *in situ* hybridization of kidneys (E10.5) with anti-sense probes for *Slit2* (A-D), *Robo2* (E-H), *and Foxc1* (I-L). *Slit2* is expressed throughout the WD, while expression of *Robo2* and *Foxc1* is widely detected in the metanephric region.